SUPLEMENTARY INFORMATION

Infrared Spectra of (*Z*)- and (*E*)-•$C_2H_3C(CH_3)I$ Radicals Produced upon Photodissociation of (*Z*)- and (*E*)- $(CH_2I)HC{=}C(CH_3)I$ in Solid *para*-Hydrogen

Karolina Anna Haupa,[†] *Kuang-Po Chen,*[†] *Yaw-Kuen Li,*[†‡] *and Yuan-Pern Lee**[†‡¶]

[†]Department of Applied Chemistry and Institute of Molecular Science, National Chiao Tung University, Hsinchu 30010, Taiwan,

[‡]Center for Emergent Functional Matter Science, National Chiao Tung University, Hsinchu 30010, Taiwan.

[¶]Institute of Atomic and Molecular Sciences, Academia Sinica, Taipei 10617, Taiwan.

E-mail: karolina.haupa@gmail.com (K.A.H.); yplee@nctu.edu.tw (Y.-P. L)

Table of contents

A. Synthetic procedure and characterization of (*Z*)-1,3-diiodobut-2-ene (3)

The (*Z*)-1,3-diiodobut-2-ene precursor was synthesized according to the following scheme.[1, 2]

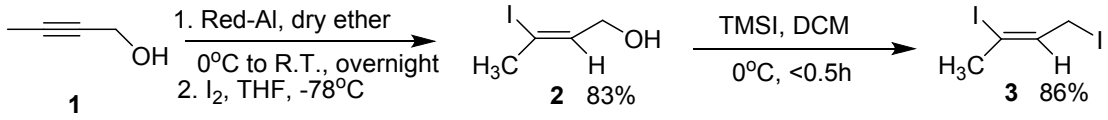

The glassware used was pre-dried. All reactions were undertaken under a N_2 atmosphere. Sodium bis(methoxyethoxy)aluminium hydride (62.0 mL, 3.5 M) in toluene (0.218 mol, 1.50 eq) was placed in a two-necked flask with a stirrer. The flask was kept in an ice bath. 2-butyn-1-ol (10.8 mL, 0.145 mole, 1eq) in Et_2O (150 mL) was then slowly added via a funnel. The reaction mixture was stirred in an ice bath for 0.5 h and near 23 °C overnight. The mixture was kept in an ice bath during addition of ethyl acetate (10 mL) to quench excess sodium bis(methoxyethoxy)aluminium hydride. The reaction was moved to a cold bath (–78 °C); a solution containing I_2 (55.0 g, 0.217 mol, 1.50 eq) in dry THF (tetrahydrofuran, 150 mL) was slowly added via a funnel. Afterward, the mixture was stirred near 23 °C and sequentially dropped in of saturated $Na_2S_2O_3$ (200 mL), saturated Rochelle salt solutions (200 mL) and ethyl acetate (100 mL). After the separation of the organic phase, the aqueous phase was extracted with ethyl acetate (3×100 mL); the combined organic extracts were dried over Na_2SO_4 and concentrated under decreased pressure. Purification of the residue with a flash chromatograph (EtOAc/Hex: 1/8, 1/6, 1/4, 1/3) gave **2** (23.6 g, 0.119 mol, 82.6 %) as a yellow oil, which was stored at -20 °C. The NMR data (^{1}H and ^{13}C) were comparable with those reported in the literature.[1]

2 (23.6 g, 0.119 mol) was placed in a flask containing DCM (CH_2Cl_2, 180 mL) as solvent. The mixture was kept in an ice bath for 20 min. TMSI (trimethylsilyl iodide) was then added dropwise to the mixture at the same temperature and stirred for another 20 min. After the reaction, the resulting solution was quenched with saturated $Na_2SO_{3(aq)}$. The solvent was removed on an evaporator; the product was purified on a column chromatograph eluted with hexane and further DCM/Hex (1/40 and 1/20). The yield of **3** was 31.6 g, 86.0 %.

The NMR data (^{1}H and ^{13}C) collected with $CDCl_3$ as solvent were comparable with those reported.[2]

The product is labile in $CDCl_3$; for this reason, CD_2Cl_2 was used as further solvent. ^{1}H-NMR (300 MHz, CD_2Cl_2): δ 5.76 (tq, J = 8.3, 1.5 Hz, 1H, CH), 3.89 (d, J = 8.3 Hz, 2H, CH_2), 2.52 (s, 3H, CH_3); ^{13}C-NMR with distortionless enhancement of polarization transfer using a 135 degree decoupler pulse (DEPT-135, 75.4MHz, CD_2Cl_2): δ 131.6 (s), 106.3 (d), 32.9 (q), 9.0 (t).

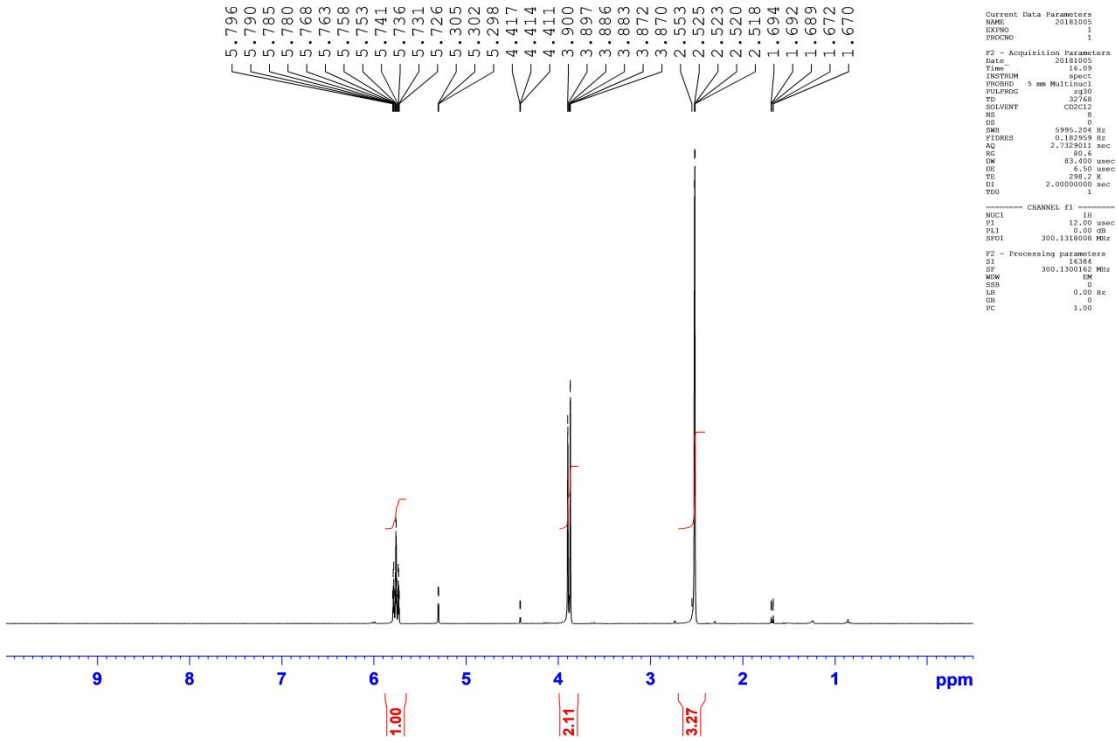

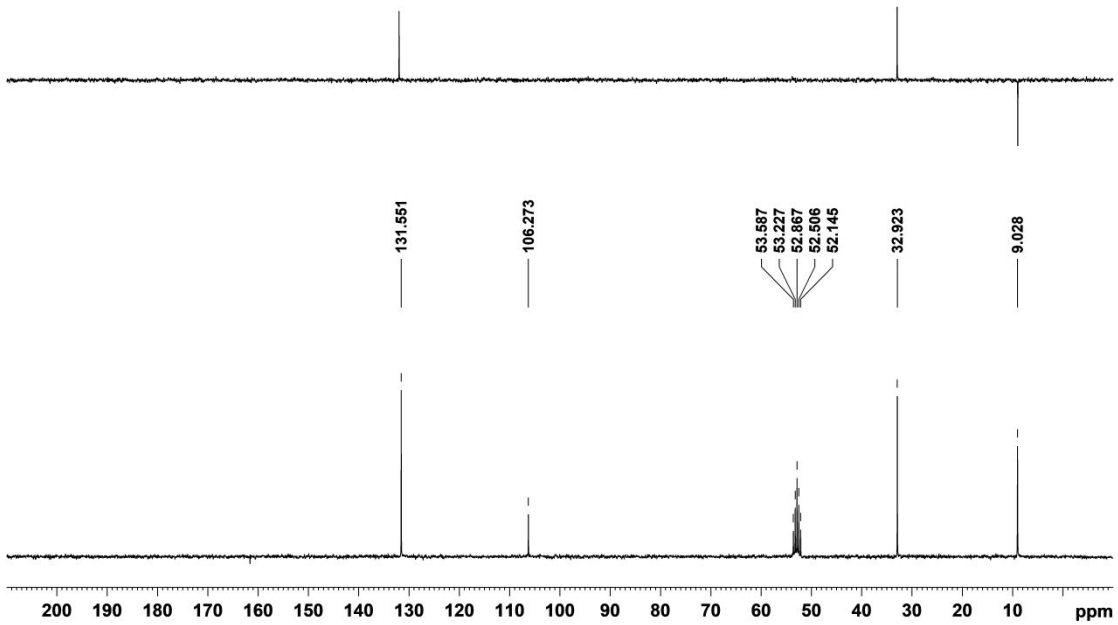

B. Synthetic procedures and characterization of (*E*)-1,3-diiodobut-2-ene (5)

The (*Z*)-1,3-diiodobut-2-ene precursor was synthesized according to the following scheme.[2, 3]

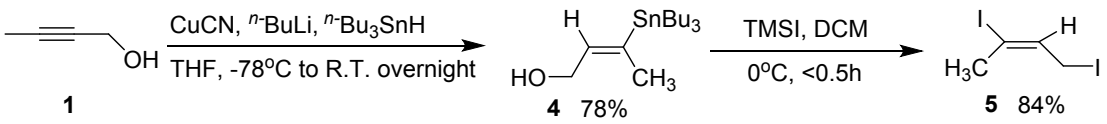

Compound **4** was synthesized based on the procedures shown in ref. **3** with minor modification in the eluent of the column chromatograph. The eluent solvent of DCM/Hex changed from 1/4, 1/3, 1/2, 2/3, to 1/1 was employed. **4** (12.0 g) was obtained, which was used directly in the next step. The NMR data of **4 were** consistent with those in the literature.

4 (5.5g, 0.028 mol) was added to THF (40 mL). The mixture was kept at 0–5 °C for 20 min. TMSI was added dropwise to the reaction mixture. The resulting solution was continuously stirred for 20 min. The work-up and purification were identical to those for **3**. Yield of **5** was 84.0% (7.2 g). The NMR data (^{1}H and ^{13}C) were consistent with those reported in the literature.[2]

^{1}H-NMR (300MHz, $CDCl_3$): δ 6.53-6.45 (m, 1H, CH), 3.78 (d, J = 9.0 Hz, 2H, CH_2), 2.42 (s, 3H, CH_3); ^{13}C-NMR (75.4MHz, CDC_3): δ 136.7 (s), 99.6 (d), 27.0 (q), -0.6 (t).

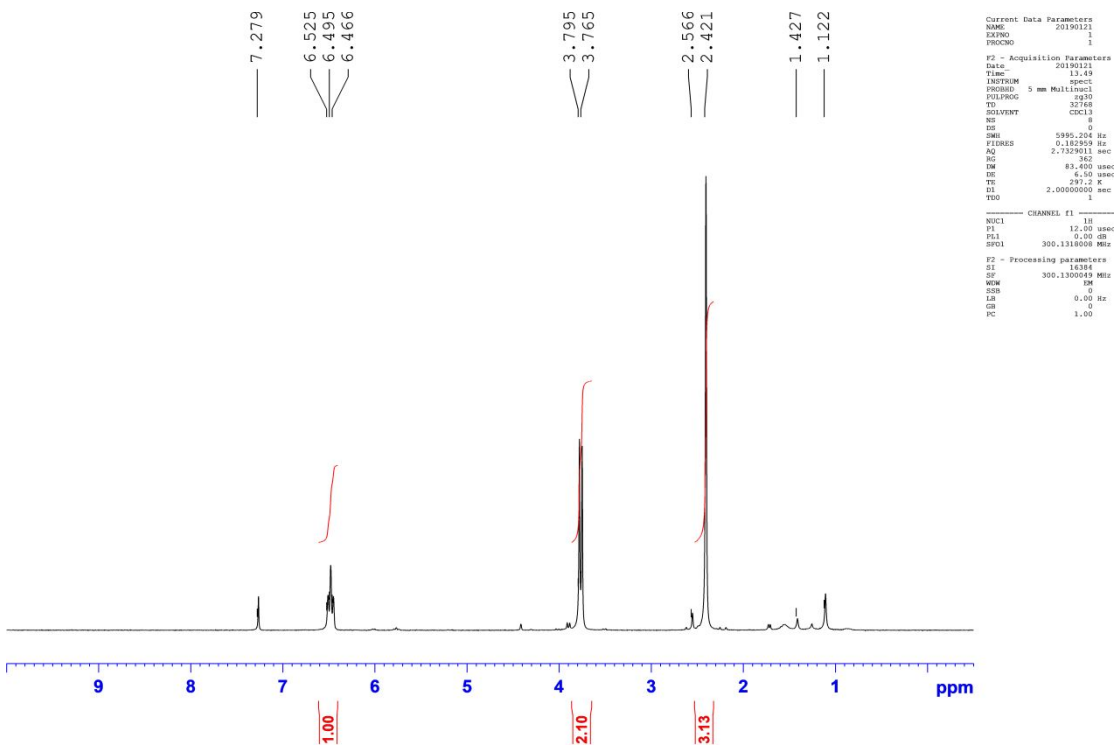

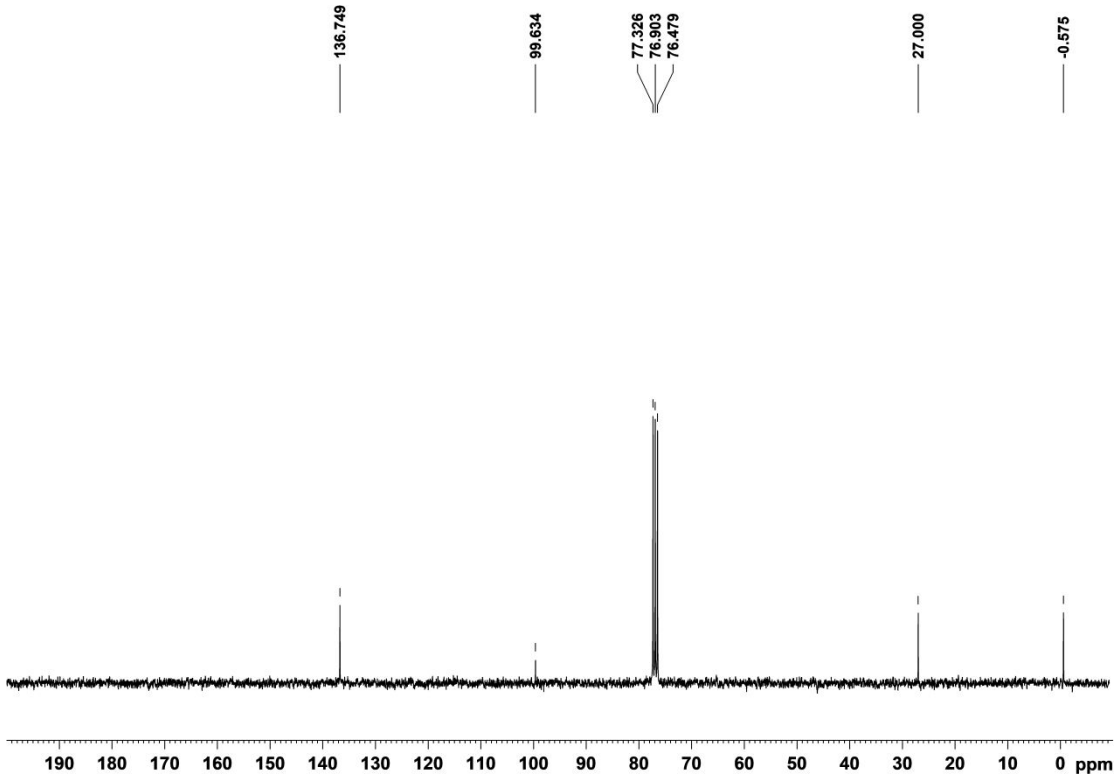
136.749
99.634
77.326
76.903
76.479
27.000
-0.575
190 180 170 160 150 140 130 120 110 100 90 80 70 60 50 40 30 20 10 0 ppm

Table S1. Comparison of observed vibrational wavenumbers and IR intensities of (*Z*)-1,3-diiodobut-2-ene (**3**) with those calculated with the B2PLYP-D3/aug-cc-pVTZ-pp method

Mode	*p*-H_2		Calculated		Mode description[c]
	ν /cm^{-1}	Int.[a]	ν[b] /cm^{-1}	Intensity /km mol^{-1}	
ν_1			3010.7	0.3	CH_2 asym. stretch
ν_2	2982.6	7	2962.3	6.6	CH stretch
ν_3			2944.0	2.4	CH_2 sym. stretch
ν_4	2972.4	18	2942.2	11.1	CH_3 asym. stretch
ν_5	2824.5	15	2932.2	5.5	CH_2 asym. stretch in CH_3
ν_6	2847.9	5	2869.4	16.7	CH_3 sym. stretch
ν_7	1641.2	20	1609.7	23.5	C=C stretch
ν_8	1439.8	3	1441.7	3.5	CH_3 scissor
ν_9	1432.0	29	1428.6	7.2	CH_2 scissor
ν_{10}	1430.3	18	1424.7	12.1	CH_3 deform
ν_{11}	1392.6	1	1370.5	1.8	CH_3 umbrella
ν_{12}	1299.1	41	1286.3	25.8	CH in-plane bend
ν_{13}	1168.6	25	1158.3	23.2	CH_2 twist
ν_{14}	1163.0	100	1145.1	67.4	CH_2 wag
ν_{15}	1095.0	<1	1084.2	1.8	$C^{(1)}C^{(2)}$& $C^{(3)}C^{(4)}$ stretchs (*op*)
ν_{16}	1061.6	31	1056.6	23.8	$C^{(3)}C^{(4)}$ stretch
ν_{17}	1038.2	<1	1044.6	0.6	CH_3 rock
ν_{18}	965.3	1	961.9	2.4	CH_3 wag
ν_{19}	837.9	27	851.9	17.6	CH out-of-plane bend
ν_{20}	810.6	8	821.6	6.1	CH_2 rock
ν_{21}	547.3	16	570.1	28.4	C1I stretch
ν_{22}	530.3	10	550.6	10.3	CCC bend (*ip*) + $C^{(3)}$I stretch
ν_{23}			457.0	2.7	$C^{(3)}$I stretch + CCC bend (*op*)
ν_{24}			445.4	11.7	CCCC out-of-plane deform
ν_{25}			333.1	1.2	$C^{(4)}C^{(3)}$I bend
ν_{26}			302.5	1.6	CCCC out-of-plane deform
ν_{27}			245.2	0.5	CH_3 torsion + $C^{(2)}C^{(3)}$I bend
ν_{28}			237.2	0.1	CH_3 torsion
ν_{29}			140.6	1.7	$C^{(2)}$C1I bend
ν_{30}			79.3	0.1	CH_2I torsion

[a] Percentage IR intensity relative to that of the most intense line. [b] Harmonic vibrational wavenumbers scaled according to $y = 0.9252\ x + 56.4$; see text. [c] *ip*: in-phase; *op*: out-of-phase. Superscript numbers in parentheses indicate atomic numbering shown in Fig. 1.

Table S2. Comparison of observed vibrational wavenumbers and IR intensities of (*E*)-1,3-diiodobut-2-ene (**5**) with those calculated with the B2PLYP-D3/aug-cc-pVTZ-pp method

Mode	*p*-H_2		Calculated		Mode description[c]
	ν /cm^{-1}	Int.[a]	ν[b] /cm^{-1}	Intensity /km mol^{-1}	
ν_1			3019.1	0.7	CH_2 asym. stretch + CH stretch
ν_2			3002.7	0.4	CH stretch + CH_2 asym. stretch
ν_3	2992.0	4	2955.0	12.7	CH_3 stretch + CH_2 sym. stretch
ν_4			2948.7	3.6	CH_2 sym. stretch + CH_3 stretch
ν_5			2933.9	3.6	CH_2 asym. stretch in CH_3
ν_6			2876.8	8.7	CH_3 sym. stretch
ν_7	1629.9	30	1599.5	51.6	C=C stretch
ν_8	1465.6	5	1448.5	6.6	CH_2 scissoring + CH_3 deform
ν_9	1452.4	5	1428.1	3.7	CH_3 deform + CH_2 scissoring
ν_{10}	1429.5	10	1425.1	10.6	CH_3 deform + CH_2 scissoring
ν_{11}	1381.6	7	1372.0	6.6	CH_3 umbrella
ν_{12}	1334.8	1	1322.1	2.2	CH bend
ν_{13}	1150.1 /1153.0	100	1147.0	20.4	$HC^{(1)}C^{(2)}$ bend
ν_{14}			1139.9	101.9	CH_2 wagg
ν_{15}	1070.7	4	1064.6	16.1	CH_3 wag
ν_{16}	1060.4	36	1052.7	28.1	$C^{(1)}C^{(2)}$ & $C^{(3)}C^{(4)}$ stretchs (*op*)
ν_{17}			1040.8	1.5	CH_3 rock
ν_{18}	928.8	3	927.0	2.9	$C^{(1)}C^{(2)}$ & $C^{(3)}C^{(4)}$ stretchs (*ip*)
ν_{19}	859.4	16	875.8	13.8	CH out-of-plane bend
ν_{20}			841.1	0.5	CH_2 rock
ν_{21}	611.5	4	628.2	7.8	CCC bend (*op*)
ν_{22}			546.1	19.8	C1I stretch
ν_{23}			454.0	22.2	CCCC out-of-plane deform
ν_{24}			392.1	8.8	$C(CH_2)C$ bend + CI stretch
ν_{25}			332.4	2.4	CCC bend (*ip*)
ν_{26}			297.5	0.2	$C^{(3)}C^{(4)}I$ bend
ν_{27}			243.2	0.3	out-of-plane deform + CH_3 torsion
ν_{28}			196.9	0.1	CH_3 torsion
ν_{29}			101.9	0.4	$C^{(2)}C^{(1)}I$ bend
ν_{30}			87.9	0.7	CH_2I torsion

[a] Percentage IR intensity relative to that of the most intense line. [b] Harmonic vibrational wavenumber scaled according to $y = 0.9252\ x + 56.4$; see text. [c] *ip*: in-phase; *op*: out-of-phase. Superscript numbers in parentheses indicate atomic numbering shown in Fig. 1.

Table S3. Vibrational wavenumbers and IR intensities of (*Z*)-(CH_2I)HC=C(CH_3)• **(7)** and (*E*)-(CH_2I)HC=C(CH_3)• **(9)** calculated with the B2PLYP-D3/aug-cc-pVTZ-pp method

Mode	(*Z*)-(CH_2I)HC=C(CH_3)•		(*E*)-(CH_2I)HC=C(CH_3)•	
	ν^a / cm^{-1}	Int. / km mol^{-1}	ν^a / cm^{-1}	Int. / km mol^{-1}
ν_1	3009.7	0.2	3189.1	0.6
ν_2	2941.7	4.3	3142.7	1.6
ν_3	2933.0	5.2	3117.7	4.3
ν_4	2908.9	10.5	3109.1	4.8
ν_5	2884.5	9.6	3081.5	10.3
ν_6	2829.5	19.3	2997.7	14.0
ν_7	1691.2	25.9	1757.6	22.0
ν_8	1431.8	12.4	1490.3	11.4
ν_9	1427.7	1.8	1476.9	4.8
ν_{10}	1412.9	8.7	1467.4	7.0
ν_{11}	1356.9	2.3	1405.5	4.6
ν_{12}	1266.0	0.4	1326.2	1.4
ν_{13}	1152.7	74.8	1182.9	67.1
ν_{14}	1132.7	4.0	1146.4	6.6
ν_{15}	1070.7	2.9	1060.9	0.1
ν_{16}	1032.2	0.8	1052.1	0.4
ν_{17}	1022.0	1.2	1037.7	2.9
ν_{18}	914.1	6.5	909.8	6.6
ν_{19}	825.2	4.3	840.2	9.9
ν_{20}	781.7	19.1	802.4	36.6
ν_{21}	555.1	29.4	554.0	32.5
ν_{22}	463.4	0.9	482.7	0.7
ν_{23}	291.5	3.1	372.2	12.5
ν_{24}	284.1	8.3	212.5	0.5
ν_{25}	244.2	5.8	197.7	2.2
ν_{26}	179.4	2.0	114.1	0.0
ν_{27}	122.4	0.2	49.0	0.7

[a] Harmonic vibrational wavenumber scaled according to $y = 0.9252\,x + 56.4$; see text.

Table S4. Vertical excitation energies (ΔE) and oscillator strengths of the first six singlet transitions of (*Z*)-1,3-diiodobut-2-ene **(3)** calculated with the TD-B3LYP/aug-cc-pVTZ-pp method

#	ΔE / nm	Oscillator strength	Assignment[a]
1	302.5	0.0418	HOMO → LUMO (65)
			HOMO-2 → LUMO (31)
2	300.8	0.0023	HOMO-1 → LUMO (95)
3	280.5	0.0076	HOMO → LUMO+1 (84)
4	275.6	0.1394	HOMO-2 → LUMO (60)
			HOMO → LUMO (29)
5	261.5	0.0014	HOMO-3 → LUMO (97)
6	248.2	0.0040	HOMO-3 → LUMO+1 (64)
			HOMO-2 → LUMO (29)

[a] Transitions with contribution greater than 10% are listed.

Table S5. Vertical excitation energies (ΔE) and oscillator strengths of the first six singlet transitions of (*E*)-1,3-diiodobut-2-ene **(5)** calculated with the TD-B3LYP/aug-cc-pVTZ-pp method

#	ΔE / nm	Oscillator strength	Assignment[a]
1	306.6	0.0789	HOMO → LUMO (61)
			HOMO-2 → LUMO (25)
2	300.8	0.0042	HOMO-1 → LUMO (90)
3	290.7	0.0242	HOMO → LUMO+1 (45)
			HOMO-1 → LUMO (44)
4	276.2	0.1611	HOMO → LUMO+1 (46)
			HOMO → LUMO (25)
			HOMO-2 → LUMO (24)
5	267.5	0.0086	HOMO-3 → LUMO (93)
6	249.2	0.0001	HOMO-3 → LUMO+1 (82)

[a] Transitions with contribution greater than 10% are listed.

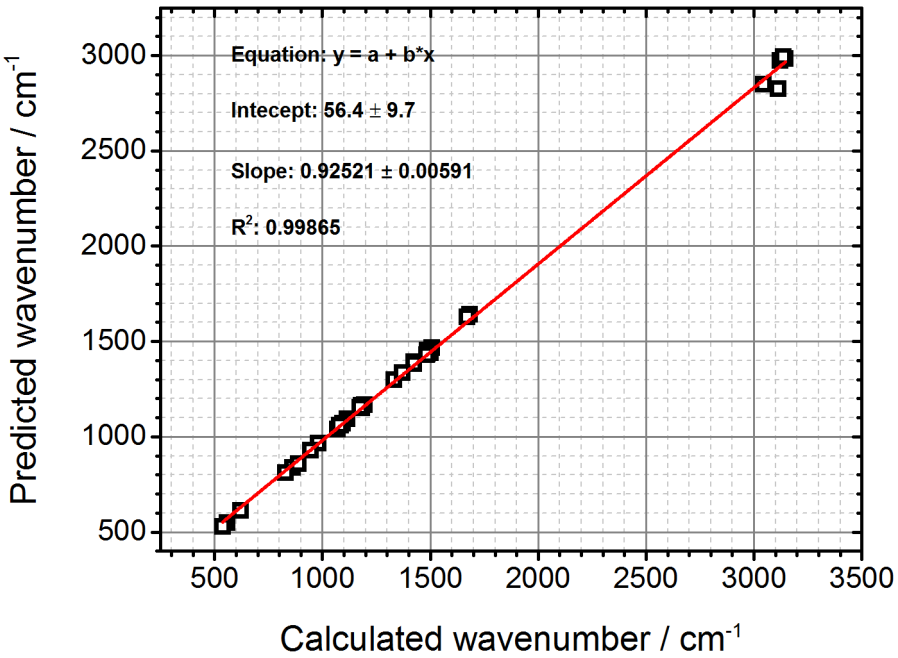

Figure S1. Linear fit of experimental wavenumbers versus harmonic vibrational wavenumbers of (*Z*)-1,3-diiodobut-2-ene **(3)** and (*Z*)-1,3-diiodobut-2-ene **(5)** calculated with the B2PLYP-D3/aug-cc-pVTZ-pp method.

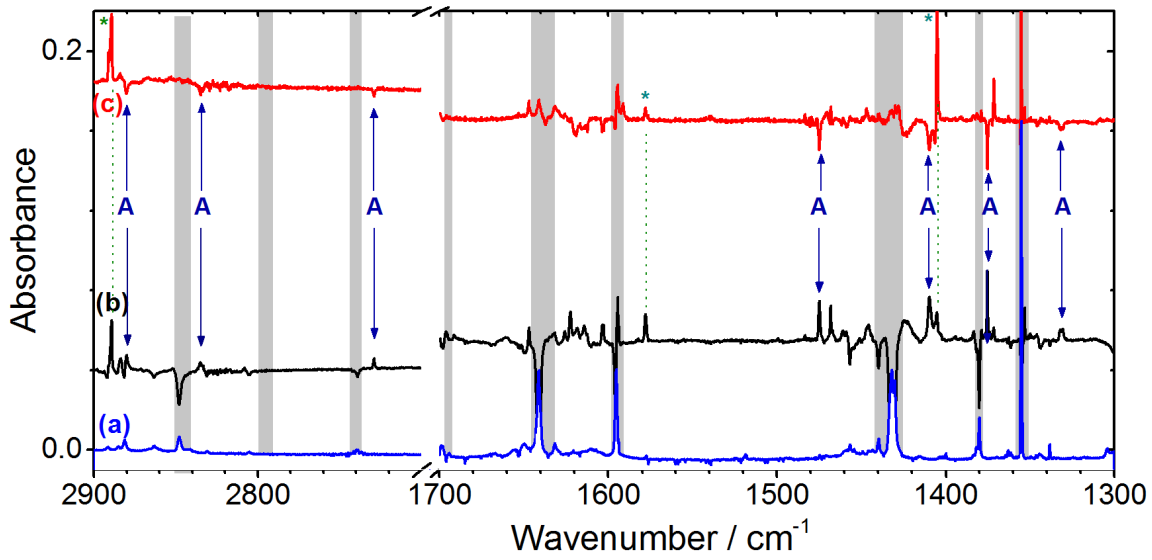

Figure S2. Infrared spectra of (*Z*)-1,3-diiodobut-2-ene **(3)** matrix in regions 2900–2700 and 1700–1300 cm^{-1} recorded at various stages of experiments. (a) Absorption spectrum after deposition at 3.3 K for 10 h. (b) Difference spectrum upon irradiation of the matrix at 280 nm for 5 min. (c) Difference spectrum after secondary photolysis at 445 nm for 10 min. Lines in group A are marked with blue arrows and labels; grey areas indicate regions in which the absorption of the parent compound or byproducts interferes severely. Unidentified lines are marked with *.

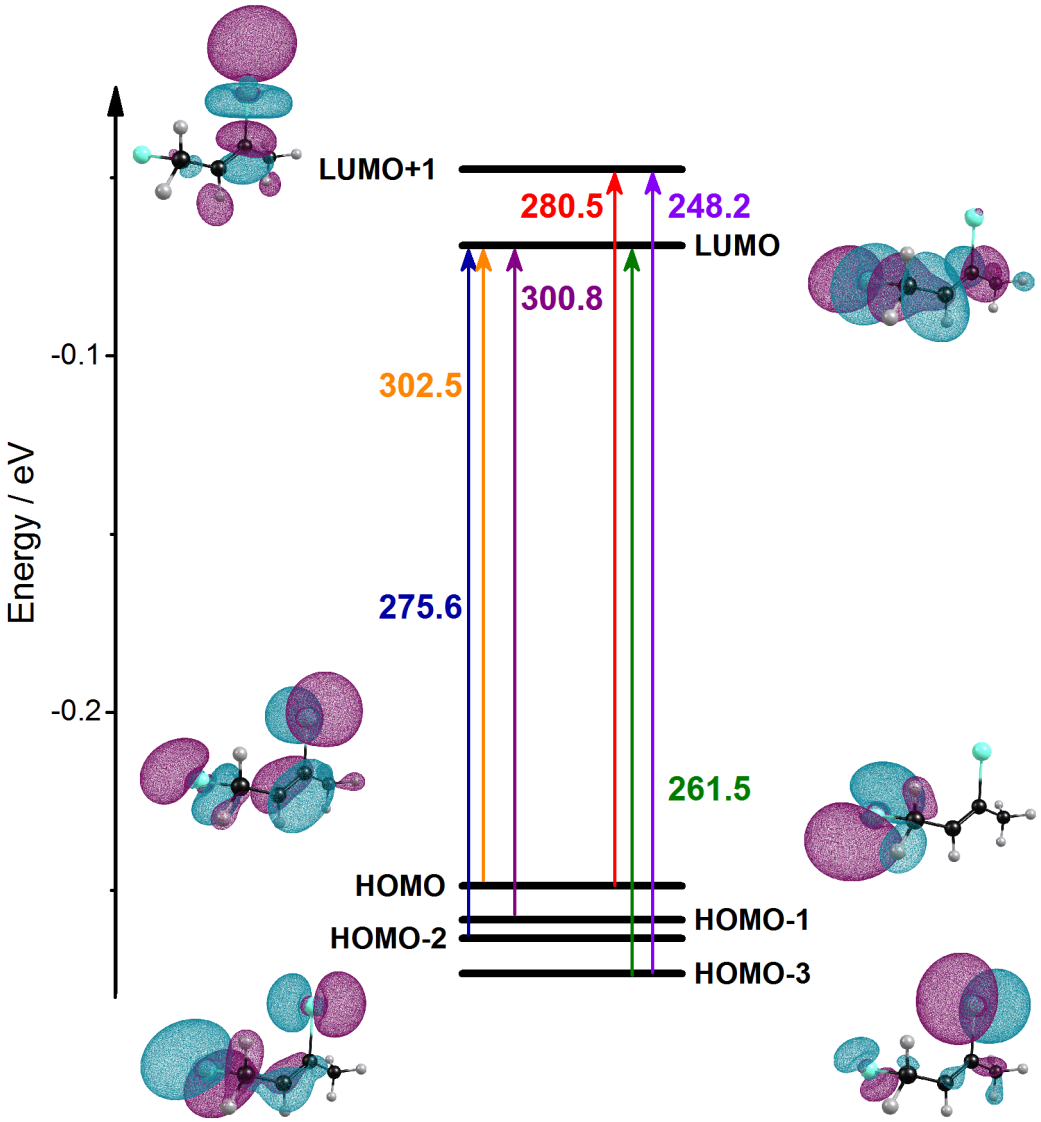

Figure S3. Molecular orbitals and electronic transitions of (*Z*)-1,3-diiodobut-2-ene **(3)** calculated with the TD-B3LYP/aug-cc-pVTZ-pp method. The frontier molecular-orbital diagram including orbital contours simulated with electron-density isovalue of 0.03 e/Å^3 are presented.

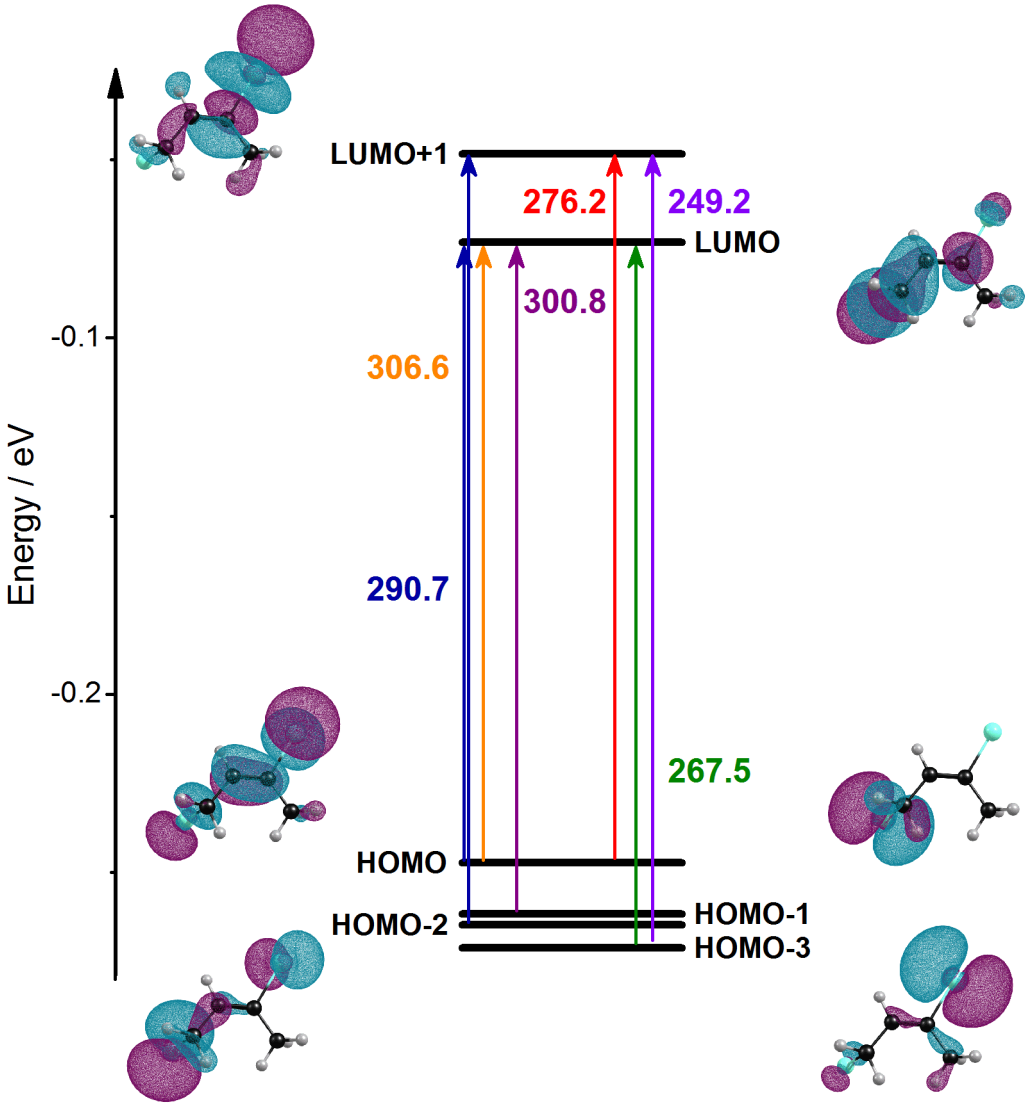

Figure S4. Molecular orbitals and electronic transitions of (*E*)-1,3-diiodobut-2-ene **(5)** calculated with the TD-B3LYP/aug-cc-pVTZ-pp method. The frontier molecular-orbital diagram including orbital contours simulated with electron-density isovalue of 0.03 e/Å^3 are presented.